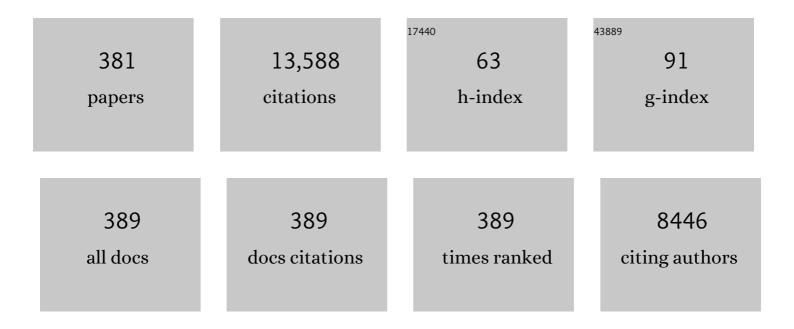
Jianzhuang Jiang

List of Publications by Year in descending order

Source: https://exaly.com/author-pdf/4437340/publications.pdf Version: 2024-02-01



#	Article	IF	CITATIONS
1	A Scalable General Synthetic Approach toward Ultrathin Imine-Linked Two-Dimensional Covalent Organic Framework Nanosheets for Photocatalytic CO ₂ Reduction. Journal of the American Chemical Society, 2019, 141, 17431-17440.	13.7	418
2	A Decade Journey in the Chemistry of Sandwich-Type Tetrapyrrolatoâ^'Rare Earth Complexes. Accounts of Chemical Research, 2009, 42, 79-88.	15.6	328
3	Sandwich-type heteroleptic phthalocyaninato and porphyrinato metal complexes. Chemical Society Reviews, 1997, 26, 433.	38.1	267
4	Two-Dimensional Covalent Organic Frameworks with Cobalt(II)-Phthalocyanine Sites for Efficient Electrocatalytic Carbon Dioxide Reduction. Journal of the American Chemical Society, 2021, 143, 7104-7113.	13.7	198
5	High Performance Organic Field-Effect Transistors Based on Amphiphilic Tris(phthalocyaninato) Rare Earth Triple-Decker Complexes. Journal of the American Chemical Society, 2005, 127, 15700-15701.	13.7	194
6	Postsynthetic Metalation of a Robust Hydrogen-Bonded Organic Framework for Heterogeneous Catalysis. Journal of the American Chemical Society, 2019, 141, 8737-8740.	13.7	178
7	Vibrational spectroscopy of phthalocyanine and naphthalocyanine in sandwich-type (na)phthalocyaninato and porphyrinato rare earth complexes. Coordination Chemistry Reviews, 2006, 250, 424-448.	18.8	174
8	Single-molecule magnetism of tetrapyrrole lanthanide compounds with sandwich multiple-decker structures. Coordination Chemistry Reviews, 2016, 306, 195-216.	18.8	172
9	Electron-Donating or -Withdrawing Nature of Substituents Revealed by the Electrochemistry of Metal-Free Phthalocyanines. Inorganic Chemistry, 2006, 45, 2327-2334.	4.0	169
10	Tuning the Valence of the Cerium Center in (Na)phthalocyaninato and Porphyrinato Cerium Double-Deckers by Changing the Nature of the Tetrapyrrole Ligands. Journal of the American Chemical Society, 2003, 125, 12257-12267.	13.7	158
11	Morphology Controlled Self-Assembled Nanostructures of Sandwich Mixed (Phthalocyaninato)(Porphyrinato) Europium Triple-Deckers. Effect of Hydrogen Bonding on Tuning the Intermolecular Interaction. Journal of the American Chemical Society, 2008, 130, 11623-11630.	13.7	146
12	Morphology-Controlled Self-Assembled Nanostructures of 5,15-Di[4-(5-acetylsulfanylpentyloxy)phenyl]porphyrin Derivatives. Effect of Metalâ^Ligand Coordination Bonding on Tuning the Intermolecular Interaction. Journal of the American Chemical Society, 2008, 130, 17044-17052.	13.7	145
13	Co(II) Metalâ `Organic Frameworks (MOFs) Assembled from Asymmetric Semirigid Multicarboxylate Ligands: Synthesis, Crystal Structures, and Magnetic Properties. Crystal Growth and Design, 2009, 9, 5273-5282.	3.0	124
14	Synthesis, spectroscopic and electrochemical properties of substituted bis(phthalocyaninato)lanthanide(III) complexes. Polyhedron, 1997, 16, 515-520.	2.2	116
15	Twist angle perturbation on mixed (phthalocyaninato)(porphyrinato) dysprosium(iii) double-decker SMMs. Chemical Communications, 2012, 48, 2973.	4.1	113
16	Highâ€Performance Airâ€Stable Ambipolar Organic Fieldâ€Effect Transistor Based on Tris(phthalocyaninato) Europium(III). Advanced Materials, 2012, 24, 1755-1758.	21.0	111
17	Fabrication of a Hydrogenâ€Bonded Organic Framework Membrane through Solution Processing for Pressureâ€Regulated Gas Separation. Angewandte Chemie - International Edition, 2020, 59, 3840-3845.	13.8	109
18	Facile approaches to build ordered amphiphilic tris(phthalocyaninato) europium triple-decker complex thin films and their comparative performances in ozone sensing. Physical Chemistry Chemical Physics, 2010, 12, 12851	2.8	106

#	Article	IF	CITATIONS
19	Tetrapyrrole macrocycle based conjugated two-dimensional mesoporous polymers and covalent organic frameworks: From synthesis to material applications. Coordination Chemistry Reviews, 2019, 378, 188-206.	18.8	106
20	Synthesis, Structure, Spectroscopic Properties, and Electrochemistry of Rare Earth Sandwich Compounds with Mixed 2,3-Naphthalocyaninato and Octaethylporphyrinato Ligands. Chemistry - A European Journal, 2001, 7, 5059-5069.	3.3	103
21	Multifunctional Tubular Organic Cageâ€Supported Ultrafine Palladium Nanoparticles for Sequential Catalysis. Angewandte Chemie - International Edition, 2019, 58, 18011-18016.	13.8	103
22	8-Hydroxyquinoline-Substituted Boron–Dipyrromethene Compounds: Synthesis, Structure, and OFF–ON–OFF Type of pH-Sensing Properties. Journal of Organic Chemistry, 2011, 76, 3774-3781.	3.2	101
23	Facile preparation of N-doped corncob-derived carbon nanofiber efficiently encapsulating Fe2O3 nanocrystals towards high ORR electrocatalytic activity. Journal of Energy Chemistry, 2020, 44, 121-130.	12.9	100
24	Elucidating heterogeneous photocatalytic superiority of microporous porphyrin organic cage. Nature Communications, 2020, 11, 1047.	12.8	100
25	Post-synthetic modification of porous organic cages. Chemical Society Reviews, 2021, 50, 8874-8886.	38.1	98
26	Infra-red spectra of phthalocyanine and naphthalocyanine in sandwich-type (na)phthalocyaninato and porphyrinato rare earth complexes. Polyhedron, 1999, 18, 2129-2139.	2.2	96
27	Tuning the morphology of self-assembled nanostructures of amphiphilic tetra(p-hydroxyphenyl)porphyrins with hydrogen bonding and metal–ligand coordination bonding. Journal of Materials Chemistry, 2009, 19, 2417.	6.7	94
28	Comparative Electrochemical Study of Unsubstituted and Substituted Bis(phthalocyaninato) Rare Earth(III) Complexes. European Journal of Inorganic Chemistry, 2004, 2004, 510-517.	2.0	92
29	Controlling the Nature of Mixed (Phthalocyaninato)(porphyrinato) Rare-Earth(III) Double-Decker Complexes: The Effects of Nonperipheral Alkoxy Substitution of the Phthalocyanine Ligand. Chemistry - A European Journal, 2006, 12, 1475-1485.	3.3	90
30	Rational enhancement of the energy barrier of bis(tetrapyrrole) dysprosium SMMs via replacing atom of porphyrin core. Chemical Science, 2015, 6, 5947-5954.	7.4	90
31	Heteroleptic Bis(Phthalocyaninato) Europium(III) Complexes Fused with Different Numbers of 15-Crown-5 Moieties. Synthesis, Spectroscopy, Electrochemistry, and Supramolecular Structure. Inorganic Chemistry, 2006, 45, 3794-3802.	4.0	88
32	Exfoliation of amorphous phthalocyanine conjugated polymers into ultrathin nanosheets for highly efficient oxygen reduction. Journal of Materials Chemistry A, 2019, 7, 3112-3119.	10.3	87
33	Sandwich-type tetrakis(phthalocyaninato) dysprosium–cadmium quadruple-decker SMM. Chemical Communications, 2011, 47, 9624.	4.1	86
34	Infrared spectra of phthalocyanine and naphthalocyanine in sandwich-type (na)phthalocyaninato and porphyrinato rare earth complexes. Part 3. The effects of substituents and molecular symmetry on the infrared characteristics of phthalocyanine in bis(phthalocyaninato) rare earth complexes. Spectrochimica Acta - Part A: Molecular and Biomolecular Spectroscopy, 2003, 59, 3273-3286.	3.9	84
35	Electron-Donating Alkoxy-Group-Driven Synthesis of Heteroleptic Tris(phthalocyaninato) Lanthanide(III) Triple-Deckers with Symmetrical Molecular Structure. Chemistry - A European Journal, 2005, 11, 1425-1432.	3.3	83
36	Robust Biological Hydrogenâ€Bonded Organic Framework with Postâ€Functionalized Rhenium(I) Sites for Efficient Heterogeneous Visibleâ€Lightâ€Driven CO ₂ Reduction. Angewandte Chemie - International Edition, 2021, 60, 8983-8989.	13.8	83

#	Article	IF	CITATIONS
37	Maximizing Electroactive Sites in a Threeâ€Dimensional Covalent Organic Framework for Significantly Improved Carbon Dioxide Reduction Electrocatalysis. Angewandte Chemie - International Edition, 2022, 61, .	13.8	83
38	Efficient ORR electrocatalytic activity of peanut shell-based graphitic carbon microstructures. Journal of Materials Chemistry A, 2018, 6, 12018-12028.	10.3	81
39	Rational Modification of Two-Dimensional Donor–Acceptor Covalent Organic Frameworks for Enhanced Visible Light Photocatalytic Activity. ACS Applied Materials & Interfaces, 2021, 13, 27041-27048.	8.0	80
40	Tuning Interactions between Ligands in Self-Assembled Double-Decker Phthalocyanine Arrays. Journal of the American Chemical Society, 2006, 128, 10984-10985.	13.7	79
41	Mesoporous Polyimideâ€Linked Covalent Organic Framework with Multiple Redoxâ€Active Sites for Highâ€Performance Cathodic Li Storage. Angewandte Chemie - International Edition, 2022, 61, .	13.8	79
42	Double-decker Yttrium(III) Complexes with Phthalocyaninato and Porphyrinato Ligands. Journal of Porphyrins and Phthalocyanines, 1999, 03, 322-328.	0.8	77
43	Sandwich-Type Mixed Tetrapyrrole Rare-Earth Triple-Decker Compounds. Effect of the Coordination Geometry on the Single-Molecule-Magnet Nature. Inorganic Chemistry, 2013, 52, 8505-8510.	4.0	77
44	An ultrafast responsive NO ₂ gas sensor based on a hydrogen-bonded organic framework material. Chemical Communications, 2020, 56, 703-706.	4.1	77
45	Transformation of Porous Organic Cages and Covalent Organic Frameworks with Efficient Iodine Vapor Capture Performance. Journal of the American Chemical Society, 2022, 144, 12390-12399.	13.7	77
46	A hybrid of g-C ₃ N ₄ and porphyrin-based covalent organic frameworks <i>via</i> liquid-assisted grinding for enhanced visible-light-driven photoactivity. Dalton Transactions, 2019, 48, 14989-14995.	3.3	76
47	Heterobimetallic porphyrin-based single-chain magnet constructed from manganese(iii)-porphyrin and trans-dicyanobis(acetylacetonato) ruthenate(iii) containing co-crystallized bulk anions and cations. Chemical Communications, 2010, 46, 3550.	4.1	75
48	Binuclear Phthalocyanineâ€Based Sandwichâ€Type Rare Earth Complexes: Unprecedented Two Ï€â€Bridged Biradicalâ€Metal Integrated SMMs. Chemistry - A European Journal, 2013, 19, 11162-11166.	3.3	74
49	Magneto-chiral dichroism in chiral mixed (phthalocyaninato)(porphyrinato) rare earth triple-decker SMMs. Inorganic Chemistry Frontiers, 2014, 1, 167.	6.0	74
50	Good Suzuki-coupling reaction performance of Pd immobilized at the metal-free porphyrin-based covalent organic framework. Microporous and Mesoporous Materials, 2015, 214, 108-114.	4.4	74
51	Porphyrin–Alkaline Earth MOFs with the Highest Adsorption Capacity for Methylene Blue. Chemistry - A European Journal, 2016, 22, 6345-6352.	3.3	74
52	Diverse Ni(<scp>ii</scp>) MOFs constructed from asymmetric semi-rigid V-shaped multicarboxylate ligands: structures and magnetic properties. CrystEngComm, 2010, 12, 1096-1102.	2.6	73
53	Title is missing!. Australian Journal of Chemistry, 2000, 53, 131.	0.9	72
54	Infrared spectra of phthalocyanine and naphthalocyanine in sandwich-type (na)phthalocyaninato and porphyrinato rare earth complexes. Vibrational Spectroscopy, 2003, 32, 175-184.	2.2	71

#	Article	IF	CITATIONS
55	An ethynyl-linked Fe/Co heterometallic phthalocyanine conjugated polymer for the oxygen reduction reaction. Journal of Materials Chemistry A, 2018, 6, 8349-8357.	10.3	71
56	Structures and Properties of 1,8,15,22-Tetrasubstituted Phthalocyaninato-Lead Complexes:Â The Substitutional Effect Study Based on Density Functional Theory Calculations. Journal of Physical Chemistry A, 2005, 109, 6363-6370.	2.5	69
57	Rational Design and Synthesis for Versatile FRET Ratiometric Sensor for Hg ²⁺ and Fe ²⁺ : A Flexible 8-Hydroxyquinoline Benzoate Linked Bodipy-Porphyrin Dyad. Organic Letters, 2011, 13, 5774-5777.	4.6	69
58	Thin-Film Transistors Based on Langmuirâ^'Blodgett Films of Heteroleptic Bis(phthalocyaninato) Rare Earth Complexes. Langmuir, 2005, 21, 6527-6531.	3.5	68
59	Synthesis, Characterization, and OFET Properties of Amphiphilic Heteroleptic Tris(phthalocyaninato) Europium(III) Complexes with Hydrophilic Poly(oxyethylene) Substituents. Inorganic Chemistry, 2007, 46, 11397-11404.	4.0	68
60	Air-stable ambipolar field-effect transistor based on a solution-processed octanaphthoxy-substituted tris(phthalocyaninato) europium semiconductor with high and balanced carrier mobilities. Chemical Science, 2015, 6, 1967-1972.	7.4	68
61	A Solid Transformation into Carboxyl Dimers Based on a Robust Hydrogenâ€Bonded Organic Framework for Propyne/Propylene Separation. Angewandte Chemie - International Edition, 2021, 60, 25942-25948.	13.8	68
62	Sandwich complexes of naphthalocyanine with the rare earth metals. Journal of Porphyrins and Phthalocyanines, 2003, 07, 459-473.	0.8	67
63	Amphiphilic Perylenetretracarboxyl Diimide Dimer and Its Application in Field Effect Transistor. Langmuir, 2007, 23, 5836-5842.	3.5	66
64	Synthesis, Structure, Spectroscopic Properties, and Electrochemistry of (1,8,15,22-Tetrasubstituted) Tj ETQq0 0	0 rgBT /Ov 4:0	verlock 10 Tf ! 64
65	Effect of Peripheral Hydrophobic Alkoxy Substitution on the Organic Field Effect Transistor Performance of Amphiphilic Tris(phthalocyaninato) Europium Triple-Decker Complexes. Langmuir, 2007, 23, 12549-12554.	3.5	64
66	A cruciform phthalocyanine pentad-based NIR-II photothermal agent for highly efficient tumor ablation. Chemical Science, 2019, 10, 8246-8252.	7.4	64
67	Design, Synthesis, Characterization, and OFET Properties of Amphiphilic Heteroleptic Tris(phthalocyaninato) Europium(III) Complexes. The Effect of Crown Ether Hydrophilic Substituents. Inorganic Chemistry, 2009, 48, 45-54.	4.0	61
68	A sandwich-type phthalocyaninato metal sextuple-decker complex: synthesis and NLO properties. Chemical Communications, 2013, 49, 889-891.	4.1	61
69	Ratiometric Fluorescent Detection of Pb ²⁺ by FRET-Based Phthalocyanine-Porphyrin Dyads. Inorganic Chemistry, 2017, 56, 14533-14539.	4.0	61
70	Synthesis, spectroscopic characterisation and structure of the first chiral heteroleptic bis(phthalocyaninato) rare earth complexesElectronic supplementary information (ESI) available: 1H NMR spectrum of {SmIII(Pc)[Pc(OC5H11)4]}– in CDCl3/DMSO-d6 (1â^¶1) in the presence of a few drops of hydrazine hydrate. See http://www.rsc.org/suppdata/cc/b3/b301139a/. Chemical Communications, 2003, ,	4.1	60
71	1194-1195. Porphyrin-based multi-signal chemosensors for Pb2+ and Cu2+. Organic and Biomolecular Chemistry, 2012, 10, 4782.	2.8	60
72	Guest-tuned proton conductivity of a porphyrinylphosphonate-based hydrogen-bonded organic framework. Journal of Materials Chemistry A, 2021, 9, 2683-2688.	10.3	60

#	Article	IF	CITATIONS
73	Tetrakis(phthalocyaninato) Rareâ€Earth–Cadmium–Rareâ€Earth Quadrupleâ€Decker Sandwich SMMs: Suppression of QTM by Longâ€Distance f–f Interactions. Chemistry - A European Journal, 2012, 18, 7691-7694.	3.3	59
74	Prohibitin Is Involved in Patients with IgG4 Related Disease. PLoS ONE, 2015, 10, e0125331.	2.5	59
75	Mixed phthalocyanine-porphyrin-based conjugated microporous polymers towards unveiling the activity origin of Fe–N ₄ catalysts for the oxygen reduction reaction. Journal of Materials Chemistry A, 2018, 6, 22851-22857.	10.3	59
76	Synthesis, spectroscopic properties, and electrochemistry of heteroleptic rare earth double-decker complexes with phthalocyaninato and meso-tetrakis (4-chlorophenyl)porphyrinato ligands. New Journal of Chemistry, 2004, 28, 1116-1122.	2.8	57
77	Studies of "Pinwheel-Like―Bis[1,8,15,22-tetrakis(3-pentyloxy)phthalocyaninato] Rare Earth(III) Double-Decker Complexes. Chemistry - A European Journal, 2005, 11, 7351-7357.	3.3	56
78	Enhancement of Mass Transfer for Facilitating Industrial‣evel CO ₂ Electroreduction on Atomic NiN ₄ Sites. Advanced Energy Materials, 2021, 11, 2102152.	19.5	56
79	Amphiphilic (Phthalocyaninato) (Porphyrinato) Europium Triple-Decker Nanoribbons with Air-Stable Ambipolar OFET Performance. ACS Applied Materials & Interfaces, 2016, 8, 6174-6182.	8.0	55
80	Morphology and chirality controlled self-assembled nanostructures of porphyrin–pentapeptide conjugate: effect of the peptide secondary conformation. Journal of Materials Chemistry, 2011, 21, 8057.	6.7	54
81	Synthesis, crystal structures, and luminescent properties of Cd(<scp>ii</scp>) coordination polymers assembled from asymmetric semi-rigid V-shaped multicarboxylate ligands. CrystEngComm, 2011, 13, 279-286.	2.6	53
82	Modulation of the spectroscopic property of Bodipy derivates through tuning the molecular configuration. Photochemical and Photobiological Sciences, 2011, 10, 1030-1038.	2.9	53
83	A New Bis(phthalocyaninato) Terbium Single-Ion Magnet with an Overall Excellent Magnetic Performance. Inorganic Chemistry, 2017, 56, 13889-13896.	4.0	53
84	Three Hydrogen-Bonded Organic Frameworks with Water-Induced Single-Crystal-to-Single-Crystal Transformation and High Proton Conductivity. Crystal Growth and Design, 2020, 20, 3456-3465.	3.0	51
85	Novel imine-linked porphyrin covalent organic frameworks with good adsorption removing properties of RhB. New Journal of Chemistry, 2017, 41, 6145-6151.	2.8	50
86	Porphyrin-Based Metal–Organic Frameworks for Efficient Photocatalytic H ₂ Production under Visible-Light Irradiation. Inorganic Chemistry, 2021, 60, 3988-3995.	4.0	49
87	Optically Active Mixed Phthalocyaninato–Porphyrinato Rareâ€Earth Doubleâ€Decker Complexes: Synthesis, Spectroscopy, and Solventâ€Dependent Molecular Conformations. Chemistry - A European Journal, 2008, 14, 4667-4674.	3.3	48
88	Synthesis, Crystal Structures, and Magnetic Properties of One-Dimensional Mixed Cyanide- and Phenolate-Bridged Heterotrimetallic Complexes. Crystal Growth and Design, 2010, 10, 4231-4234.	3.0	48
89	Conformational effects, molecular orbitals, and reaction activities of bis(phthalocyaninato) lanthanum double-deckers: Density functional theory calculations. Physical Chemistry Chemical Physics, 2011, 13, 13277.	2.8	48
90	Synthesis, Structure, and Singleâ€Molecule Magnetic Properties of Rareâ€Earth Sandwich Complexes with Mixed Phthalocyanine and Schiff Base Ligands. Chemistry - A European Journal, 2013, 19, 2266-2270.	3.3	48

#	Article	IF	CITATIONS
91	(TFPP)Eu[Pc(OPh) ₈]Eu[Pc(OPh) ₈]/CuPc Two-Component Bilayer Heterojunction-Based Organic Transistors with High Ambipolar Performance. ACS Applied Materials & Interfaces, 2015, 7, 2486-2493.	8.0	48
92	New Sandwichâ€Type Phthalocyaninato–Metal Quintupleâ€Decker Complexes. Chemistry - A European Journal, 2012, 18, 1047-1049.	3.3	47
93	Lysosome-targeting ratiometric fluorescent pH probes based on long-wavelength BODIPY. Journal of Materials Chemistry B, 2018, 6, 4422-4426.	5.8	47
94	Heteroleptic Rare Earth Double-Decker Complexes with Porphyrinato and 2,3-Naphthalocyaninato Ligands â^ Preparation, Spectroscopic Characterization, and Electrochemical Studies. European Journal of Inorganic Chemistry, 2001, 2001, 413-417.	2.0	46
95	Mixed (porphyrinato)(phthalocyaninato) rare-earth(III) double-decker complexes for broadband light harvesting organic solar cells. Journal of Materials Chemistry, 2011, 21, 11131.	6.7	46
96	H-aggregation mode in triple-decker phthalocyaninato-europium semiconductors. Materials design for high-performance air-stable ambipolar organic thin film transistors. Organic Electronics, 2013, 14, 2582-2589.	2.6	46
97	Synthesis and Characterization of Mixed Phthalocyaninato andmeso-Tetrakis(4-chlorophenyl)porphyrinato Triple-Decker Complexesâ՞' Revealing the Origin of Their Electronic Absorptions. European Journal of Inorganic Chemistry, 2004, 2004, 3806-3813.	2.0	45
98	Fabrication and Electrochemical Performance of Polyoxometalate-Based Three-Dimensional Metal Organic Frameworks Containing Carbene Nanocages. ACS Applied Materials & Interfaces, 2018, 10, 16660-16665.	8.0	45
99	Surfactant-assisted synthesis and electrochemical properties of an unprecedented polyoxometalate-based metal–organic nanocaged framework. Chemical Communications, 2019, 55, 1201-1204.	4.1	45
100	Single iron atoms coordinated to g-C ₃ N ₄ on hierarchical porous N-doped carbon polyhedra as a high-performance electrocatalyst for the oxygen reduction reaction. Chemical Communications, 2020, 56, 798-801.	4.1	45
101	Synthesis, Structure, and Spectroscopic and Electrochemical Properties of Heteroleptic Bis(phthalocyaninato) Rare Earth Complexes with aC4 Symmetry. Helvetica Chimica Acta, 2004, 87, 2581-2596.	1.6	44
102	The first solution-processable n-type phthalocyaninato copper semiconductor: tuning the semiconducting nature via peripheral electron-withdrawing octyloxycarbonyl substituents. Journal of Materials Chemistry, 2011, 21, 18552.	6.7	44
103	Fabrication and electrochemical performance of unprecedented POM-based metal–carbene frameworks. Journal of Materials Chemistry A, 2017, 5, 17920-17925.	10.3	43
104	Two-Dimensional Crystal Growth and Stacking of Bis(phthalocyaninato) Rare Earth Sandwich Complexes at the 1-Phenyloctane/Graphite Interface. Journal of Physical Chemistry B, 2006, 110, 1661-1664.	2.6	42
105	Lanthanide(III) Double-Decker Complexes with Octaphenoxy- or Octathiophenoxyphthalocyaninato Ligands – Revealing the Electron-Withdrawing Nature of the Phenoxy and Thiophenoxy Groups in the Double-Decker Complexes. European Journal of Inorganic Chemistry, 2006, 2006, 3703-3709.	2.0	42
106	Porphyrin-Appended Europium(III) Bis(phthalocyaninato) Complexes: Synthesis, Characterization, and Photophysical Properties. Chemistry - A European Journal, 2007, 13, 4169-4177.	3.3	42
107	Two-Photon Excited FRET Dyads for Lysosome-Targeted Imaging and Photodynamic Therapy. Inorganic Chemistry, 2018, 57, 11537-11542.	4.0	42
108	The First Slipped Pseudo-Quadruple-Decker Complex of Phthalocyanines. Inorganic Chemistry, 2004, 43, 4740-4742.	4.0	40

#	Article	IF	CITATIONS
109	Structures and Spectroscopic Properties of Bis(phthalocyaninato) Yttrium and Lanthanum Complexes: Theoretical Study Based on Density Functional Theory Calculations. Journal of Physical Chemistry A, 2007, 111, 392-400.	2.5	40
110	Location of the Hole and Acid Proton in Neutral Nonprotonated and Protonated Mixed (Phthalocyaninato)(porphyrinato) Yttrium Doubleâ€Decker Complexes: Density Functional Theory Calculations. Chemistry - A European Journal, 2007, 13, 9503-9514.	3.3	40
111	Manipulating Double-Decker Molecules at the Liquidâ^'Solid Interface. Journal of the American Chemical Society, 2010, 132, 16460-16466.	13.7	40
112	Co-crystallized fullerene and a mixed (phthalocyaninato)(porphyrinato) dysprosium double-decker SMM. Chemical Science, 2014, 5, 3214-3220.	7.4	40
113	A Br-regulated transition metal active-site anchoring and exposure strategy in biomass-derived carbon nanosheets for obtaining robust ORR/HER electrocatalysts at all pH values. Journal of Materials Chemistry A, 2019, 7, 27089-27098.	10.3	40
114	Charge Transfer Properties of Bis(phthalocyaninato) Rare Earth (III) Complexes: Intrinsic Ambipolar Semiconductor for Field Effect Transistors. Journal of Physical Chemistry C, 2008, 112, 14579-14588.	3.1	39
115	Single-crystal-to-single-crystal transformation and proton conductivity of three hydrogen-bonded organic frameworks. Chemical Communications, 2020, 56, 15529-15532.	4.1	39
116	Synthetic, Structural, Spectroscopic, and Electrochemical Studies of Heteroleptic Tris(phthalocyaninato) Rare Earth Complexes. European Journal of Inorganic Chemistry, 2005, 2005, 2612-2618.	2.0	38
117	Solid state fluorescent functionalized-triphenylamine Bodipy detector for HCl vapor with high stability and absolute fluorescent quantum yield. Dyes and Pigments, 2016, 124, 110-119.	3.7	38
118	The lower rather than higher density charge carrier determines the NH ₃ -sensing nature and sensitivity of ambipolar organic semiconductors. Materials Chemistry Frontiers, 2018, 2, 1009-1016.	5.9	38
119	Ultrathin Phthalocyanine-Conjugated Polymer Nanosheet-Based Electrochemical Platform for Accurately Detecting H ₂ O ₂ in Real Time. ACS Applied Materials & Interfaces, 2019, 11, 11466-11473.	8.0	38
120	An active site pre-anchoring and post-exposure strategy in Fe(CN)64-@PPy derived Fe/S/N-doped carbon electrocatalyst for high performance oxygen reduction reaction and zinc-air batteries. Chemical Engineering Journal, 2021, 413, 127395.	12.7	38
121	1D to 3D Heterobimetallic Complexes Tuned by Cyanide Precursors: Synthesis, Crystal Structures, and Magnetic Properties. Inorganic Chemistry, 2014, 53, 3494-3502.	4.0	37
122	Conformation-controlled emission of AIE luminogen: a tetraphenylethene embedded pillar[5]arene skeleton. Chemical Communications, 2018, 54, 837-840.	4.1	37
123	Synthetic porphyrin chemistry in China. Science China Chemistry, 2018, 61, 511-514.	8.2	37
124	Structural studies of the whole series of lanthanide double-decker compounds with mixed 2,3-naphthalocyaninato and octaethylporphyrinato ligands. New Journal of Chemistry, 2003, 27, 844-849.	2.8	36
125	2,3,9,10,16,17,23,24-Octakis(hexylsulfonyl)phthalocyanines with good n-type semiconducting properties. Synthesis, spectroscopic, and electrochemical characteristics. Journal of Materials Chemistry, 2011, 21, 6515.	6.7	36
126	Ternary Cross-Vanadium Tetra-Capped POMOFs@PPy/RGO Nanocomposites with Hybrid Battery-Supercapacitor Behavior for Enhancing Lithium Battery Storage. ACS Sustainable Chemistry and Engineering, 2020, 8, 4667-4675.	6.7	36

#	Article	IF	CITATIONS
127	Porphyrin Coordination Polymer with Dual Photocatalytic Sites for Efficient Carbon Dioxide Reduction. ACS Applied Materials & Interfaces, 2022, 14, 8048-8057.	8.0	36
128	Heteroleptic Rare Earth Double-Decker Complexes with Naphthalocyaninato and Phthalocyaninato Ligands. General Synthesis, Spectroscopic, and Electrochemical Characteristics. Inorganic Chemistry, 2005, 44, 2114-2120.	4.0	35
129	Morphology Controlled Surface-Assisted Self-Assembled Microtube Junctions and Dendrites of Metal Free Porphyrin-Based Semiconductor. Langmuir, 2010, 26, 3678-3684.	3.5	35
130	Synthesis, crystal structures, and luminescence properties of seven tripodal imidazole-based Zn/Cd(<scp>ii</scp>) coordination polymers induced by tricarboxylates. CrystEngComm, 2014, 16, 4554-4561.	2.6	35
131	(Pc)Eu(Pc)Eu[<i>trans</i> -T(COOCH ₃) ₂ PP]/GO Hybrid Film-Based Nonenzymatic H ₂ O ₂ Electrochemical Sensor with Excellent Performance. ACS Applied Materials & Interfaces, 2016, 8, 30398-30406.	8.0	35
132	Photoresponsive Covalent Organic Frameworks with Diarylethene Switch for Tunable Singlet Oxygen Generation. Chemistry of Materials, 2022, 34, 1956-1964.	6.7	35
133	Synthesis, Characterization and OFET Properties of Amphiphilic Mixed (Phthalocyaninato)(porphyrinato)europium(III) Complexes. European Journal of Inorganic Chemistry, 2009, 2009, 954-960.	2.0	34
134	Mixed (Phthalocyaninato)(Porphyrinato) Rare Earth Double-Decker Complexes with <i>C</i> ₄ Chirality: Synthesis, Resolution, and Absolute Configuration Assignment. Inorganic Chemistry, 2009, 48, 8925-8933.	4.0	34
135	Four Dibutylamino Substituents Are Better Than Eight in Modulating the Electronic Structure and Third-Order Nonlinear-Optical Properties of Phthalocyanines. Inorganic Chemistry, 2016, 55, 3151-3160.	4.0	34
136	Porous organic cages for efficient gas selective separation and iodine capture. Chemical Engineering Journal, 2022, 428, 131129.	12.7	34
137	Mixed (phthalocyaninato)(porphyrinato) heterometal complexes with sandwich quadruple-decker molecular structure. Chemical Communications, 2011, 47, 6879.	4.1	33
138	Novel bis(phthalocyaninato) rare earth complexes with the bulky and strong electron-donating dibutylamino groups: synthesis, spectroscopy, and SMM properties. Inorganic Chemistry Frontiers, 2017, 4, 1465-1471.	6.0	32
139	A Ni/Fe-based heterometallic phthalocyanine conjugated polymer for the oxygen evolution reaction. Inorganic Chemistry Frontiers, 2020, 7, 642-646.	6.0	32
140	In-situ growth of ZnS/FeS heterojunctions on biomass-derived porous carbon for efficient oxygen reduction reaction. Journal of Energy Chemistry, 2020, 47, 79-85.	12.9	32
141	Mass production of a single-atom cobalt photocatalyst for high-performance visible-light photocatalytic CO ₂ reduction. Journal of Materials Chemistry A, 2021, 9, 26286-26297.	10.3	32
142	The Electronic Absorption Characteristics of Mixed Phthalocyaninato Porphyrinato Rare Earth(III) Triple-Deckers M2(TPyP)2(Pc). European Journal of Inorganic Chemistry, 2003, 2003, 1555-1561.	2.0	31
143	New Route toward POM[6]Catenane Members for Lithium-Ion Batteries. Crystal Growth and Design, 2017, 17, 3775-3782.	3.0	31
144	Binuclear Phthalocyanine Dimerâ€Containing Yttrium Doubleâ€Decker Ambipolar Semiconductor with Sensitive Response toward Oxidizing NO ₂ and Reducing NH ₃ . ChemElectroChem, 2018, 5, 605-609.	3.4	31

#	Article	IF	CITATIONS
145	Optically Active Homoleptic Bis(phthalocyaninato) Rare Earth Double-Decker Complexes Bearing Peripheral Chiral Menthol Moieties: Effect of Ï€â^Ï€ Interaction on the Chiral Information Transfer at the Molecular Level. Inorganic Chemistry, 2010, 49, 6628-6635.	4.0	30
146	Multifunctional Tubular Organic Cage‣upported Ultrafine Palladium Nanoparticles for Sequential Catalysis. Angewandte Chemie, 2019, 131, 18179-18184.	2.0	30
147	Maximizing Electroactive Sites in a Threeâ€dimensional Covalent Organic Framework for Significantly Improved Carbon Dioxide Reduction Electrocatalysis. Angewandte Chemie, 0, , .	2.0	30
148	2,3,9,10,16,17,24,25-Octakis(octyloxycarbonyl)phthalocyanines. Synthesis, Spectroscopic, and Electrochemical Characteristics. Inorganic Chemistry, 2007, 46, 7136-7141.	4.0	29
149	Structures and Spectroscopic Properties of Fluoroboronâ^'Subtriazaporphyrin Derivatives: Density Functional Theory Approach on the Benzo-Fusing Effect. Journal of Physical Chemistry A, 2010, 114, 1931-1938.	2.5	29
150	Sandwich-type tetrakis(phthalocyaninato) rare earth(iii)–cadmium(ii) quadruple-deckers. The effect of f-electrons. Dalton Transactions, 2013, 42, 1109-1115.	3.3	29
151	Elucidating J-Aggregation Effect in Boosting Singlet-Oxygen Evolution Using Zirconium–Porphyrin Frameworks: A Comprehensive Structural, Catalytic, and Spectroscopic Study. ACS Applied Materials & Interfaces, 2019, 11, 45118-45125.	8.0	29
152	Assembled small organic molecules for photodynamic therapy and photothermal therapy. RSC Advances, 2021, 11, 10061-10074.	3.6	29
153	Ordered Molecular Assemblies of Substituted Bis(phthalocyaninato) Rare Earth Complexes on Au(111):Â In Situ Scanning Tunneling Microscopy and Electrochemical Studies. Langmuir, 2006, 22, 2105-2111.	3.5	28
154	Organic photovoltaic cells made from sandwich-type rare earth phthalocyaninato double and triple deckers. Applied Physics Letters, 2008, 93, 073303.	3.3	28
155	A Chiral Phthalocyanine Dimer with Wellâ€Defined Supramolecular Symmetry Based on π–π Interactions. Chemistry - A European Journal, 2012, 18, 15948-15952.	3.3	28
156	Constructing Sandwich-Type Rare Earth Double-Decker Complexes with N-Confused Porphyrinato and Phthalocyaninato Ligands. Inorganic Chemistry, 2012, 51, 9265-9272.	4.0	28
157	Synthesis, self-assembly, and semiconducting properties of phenanthroline-fused phthalocyanine derivatives. Journal of Materials Chemistry, 2012, 22, 15695.	6.7	28
158	Boron–Phenylpyrrin Dyes: Facile Synthesis, Structure, and pHâ€&ensitive Properties. Chemistry - A European Journal, 2013, 19, 7342-7347.	3.3	28
159	High Sensitive Ambipolar Response towards Oxidizing NO ₂ and Reducing NH ₃ Based on Bis(phthalocyaninato) Europium Semiconductors. Chinese Journal of Chemistry, 2016, 34, 975-982.	4.9	28
160	Fabricating Bis(phthalocyaninato) Terbium SIM into Tetrakis(phthalocyaninato) Terbium SMM with Enhanced Performance through Sodium Coordination. Chemistry - A European Journal, 2018, 24, 8066-8070.	3.3	28
161	Facile sonochemical synthesis of porous and hierarchical manganese(III) oxide tiny nanostructures for super sensitive electrocatalytic detection of antibiotic (chloramphenicol) in fresh milk. Ultrasonics Sonochemistry, 2019, 58, 104648.	8.2	28
162	Electrochemistry of Heteroleptic Tris(phthalocyaninato) Rare Earth(III) Complexes. European Journal of Inorganic Chemistry, 2004, 2004, 518-523.	2.0	27

#	Article	IF	CITATIONS
163	Helical nano-structures self-assembled from dimethylaminoethyloxy-containing unsymmetrical octakis-substituted phthalocyanine derivatives. Soft Matter, 2011, 7, 3417.	2.7	27
164	The effect of pore size and layer number of metal–porphyrin coordination nanosheets on sensing DNA. Journal of Materials Chemistry C, 2019, 7, 10240-10246.	5.5	27
165	Time-dependent density functional theory studies of the electronic absorption spectra of metallophthalocyanines of group IVA. International Journal of Quantum Chemistry, 2007, 107, 952-961.	2.0	26
166	Bis[1,4,8,11,15,18,22,25-octa(butyloxyl)phthalocyaninato] rare earth double-decker complexes: synthesis, spectroscopy, and molecular structure. Dalton Transactions, 2010, 39, 1321-1327.	3.3	26
167	5,10,15,20-tetra(4-pyridyl)porphyrinato zinc coordination polymeric particles with different shapes and luminescent properties. CrystEngComm, 2012, 14, 7780.	2.6	26
168	Synthesis, crystal structures and magnetic properties of mer-cyanideiron(<scp>iii</scp>)-based 1D heterobimetallic cyanide-bridged chiral coordination polymers. Dalton Transactions, 2015, 44, 4655-4664.	3.3	26
169	A Zn Metal–Organic Framework with High Stability and Sorption Selectivity for CO2. Inorganic Chemistry, 2015, 54, 10587-10592.	4.0	26
170	Twoâ€Step Solutionâ€Processed Twoâ€Component Bilayer Phthalocyaninato Copperâ€Based Heterojunctions with Interesting Ambipolar Organic Transiting and Ethanolâ€Sensing Properties. Advanced Materials Interfaces, 2016, 3, 1600253.	3.7	26
171	Chiral Discrimination of Diamines by a Binaphthalene-Bridged Porphyrin Dimer. Inorganic Chemistry, 2017, 56, 8223-8231.	4.0	26
172	Polymorphism in the self-assembled nanostructures of a tris(phthalocyaninato) europium derivative: Phase-dependent semiconducting and NO2 sensing behaviour. Organic Electronics, 2018, 53, 127-134.	2.6	26
173	New dimeric supramolecular structure of mixed (phthalocyaninato)(porphyrinato)europium(iii) sandwiches: preparation and spectroscopic characteristicsElectronic supplementary information (ESI) available: experimental and simulated MALDI-TOF mass spectra of 3; IR spectra of 1, SM1, 3 and SM3. See http://www.rsc.org/suppdata/im/b3/b300529a/. Journal of Materials Chemistry, 2003, 13, 1333.	6.7	25
174	Synthesis, Crystal Structures, and Magnetic Properties of Cyanide-Bridged Fe(III)â^'Mn(III) Complexes Based on Manganese(III)-Porphyrin and Pyridinecarboxamide Dicyanideiron(III) Building Blocks. Crystal Growth and Design, 2009, 9, 3989-3996.	3.0	25
175	Rational design of cyanide-bridged heterometallic M(I)–Mn(II) (M = Ag, Au) one-dimensional chain complexes: synthesis, crystal structures and magnetic properties. CrystEngComm, 2009, 11, 2447.	2.6	25
176	Helical Nanostructures of an Optically Active Metalâ€Free Porphyrin with Four Optically Active Binaphthyl Moieties: Effect of Metal–Ligand Coordination on the Morphology. European Journal of Inorganic Chemistry, 2010, 2010, 4000-4008.	2.0	25
177	Solution-processed single crystal microsheets of a novel dimeric phthalocyanine-involved triple-decker for high-performance ambipolar organic field effect transistors. Chemical Communications, 2017, 53, 12754-12757.	4.1	25
178	Optimizing the gas sensing properties of sandwich-type phthalocyaninato europium complex through extending the conjugated framework. Dyes and Pigments, 2019, 161, 240-246.	3.7	25
179	A robust redox-active hydrogen-bonded organic framework for rechargeable batteries. Journal of Materials Chemistry A, 2022, 10, 1808-1814.	10.3	25
180	Covalent Microporous Polymer Nanosheets for Efficient Photocatalytic CO ₂ Conversion with H ₂ O. Small, 2022, 18, e2201314.	10.0	25

#	Article	IF	CITATIONS
181	The First Fiveâ€Memberedâ€Heterocycleâ€Fused Subphthalocyanine Analogues: Chiral Tri(benzo[<i>b</i>]thiopheno)subporphyrazines. Chemistry - A European Journal, 2014, 20, 16266-16272.	3.3	24
182	Fluorescent Phthalocyanine Assembly Distinguishes Chiral Isomers of Different Types of Amino Acids and Sugars. Langmuir, 2017, 33, 7239-7247.	3.5	24
183	Functional Supramolecular Gels Based on the Hierarchical Assembly of Porphyrins and Phthalocyanines. Frontiers in Chemistry, 2019, 7, 336.	3.6	24
184	Coordination Field Tuned Cyanide-Bridged Polynuclear and One-Dimensional Heterobimetallic Complexes: Synthesis, Crystal Structures, and Magnetic Properties. Crystal Growth and Design, 2016, 16, 5753-5761.	3.0	23
185	Robust Biological Hydrogenâ€Bonded Organic Framework with Postâ€Functionalized Rhenium(I) Sites for Efficient Heterogeneous Visibleâ€Lightâ€Driven CO ₂ Reduction. Angewandte Chemie, 2021, 133, 9065-9071.	2.0	23
186	Synthesis, Spectroscopic, and Electrochemical Properties of Homoleptic Bis(Substituted-Phthalocyaninato) Cerium(IV) Complexes. Molecular Crystals and Liquid Crystals, 1999, 337, 385-388.	0.3	22
187	Inner hydrogen atom transfer in benzo-fused low symmetrical metal-free tetraazaporphyrin and phthalocyanine analogues: Density functional theory studies. Journal of Molecular Graphics and Modelling, 2009, 27, 693-700.	2.4	22
188	Synthesis and spectroscopic properties of chiral binaphthyl-linked subphthalocyanines. Chemical Communications, 2014, 50, 7663-7665.	4.1	22
189	Peripheral Substitution: An Easy Way to Tuning the Magnetic Behavior of Tetrakis(phthalocyaninato) Dysprosium(III) SMMs. Scientific Reports, 2015, 5, 8838.	3.3	22
190	Low-temperature scanning tunneling microscopy study on the electronic properties of a double-decker DyPc2 molecule at the surface. Physical Chemistry Chemical Physics, 2015, 17, 27019-27026.	2.8	22
191	Neo-N-confused Phlorins and Phlorinone: Rational Synthesis and Tunable Properties. Organic Letters, 2017, 19, 650-653.	4.6	22
192	Vibrational spectroscopic characteristics of phthalocyanine and naphthalocyanine in sandwich-type phthalocyaninato and porphyrinato rare earth complexes. Part 11—Raman spectroscopic characteristics of phthalocyanine in mixed [tetrakis(4-chlorophenyl)porphyrinato](phthalocyaninato) rare earth double-deckers. Journal of	2.5	21
193	Raman Spectroscopy, 2004, 35, 860-868. Sandwichâ€Type Heteroleptic <i>opposite</i> â€(Diazaporphyrinato)cerium Complexes: Synthesis, Spectroscopy, Structure, and Electrochemistry. European Journal of Inorganic Chemistry, 2008, 2008, 5519-5523.	2.0	21
194	Synthesis and Hollowâ€5phere Nanostructures of Optically Active Metalâ€Free Phthalocyanine. European Journal of Inorganic Chemistry, 2008, 2008, 4255-4261.	2.0	21
195	Linkage Dependence of Intramolecular Fluorescence Quenching Process in Porphyrin-Appended Mixed (Phthalocyaninato)(Porphyrinato) Yttrium(III) Double-Decker Complexes. Journal of Physical Chemistry B, 2010, 114, 13143-13151.	2.6	21
196	Planar Binuclear Phthalocyanine-Containing Sandwich-Type Rare-Earth Complexes: Synthesis, Spectroscopy, Electrochemistry, and NLO Properties. European Journal of Inorganic Chemistry, 2014, 2014, 1546-1551.	2.0	21
197	Identification of prohibitin as an antigen in Behcet's disease. Biochemical and Biophysical Research Communications, 2014, 451, 389-393.	2.1	21
198	A cross-linked supramolecular polymer constructed from pillar[5]arene and porphyrine via host–guest interactions. Polymer Chemistry, 2015, 6, 5015-5020.	3.9	21

#	Article	IF	CITATIONS
199	A cascade surface immobilization strategy to access high-density and closely distanced atomic Pt sites for enhancing alkaline hydrogen evolution reaction. Journal of Materials Chemistry A, 2020, 8, 5255-5262.	10.3	21
200	Atomic Zn Sites on N and S Codoped Biomass-Derived Graphene for a High-Efficiency Oxygen Reduction Reaction in both Acidic and Alkaline Electrolytes. ACS Applied Energy Materials, 2021, 4, 2481-2488.	5.1	21
201	Chiral bis(phthalocyaninato) terbium double-decker compounds with enhanced single-ion magnetic behavior. Inorganic Chemistry Frontiers, 2018, 5, 939-943.	6.0	20
202	Hierarchical Assembly of <scp>l</scp> -Phenylalanine-Terminated Bolaamphiphile with Porphyrin Show Tunable Nanostructures and Photocatalytic Properties. ACS Omega, 2018, 3, 10638-10646.	3.5	20
203	Multi-component supramolecular gels induce protonation of a porphyrin exciplex to achieve improved collective optical properties for effective photocatalytic hydrogen generation. Chemical Communications, 2020, 56, 527-530.	4.1	20
204	Fabrication of a Hydrogenâ€Bonded Organic Framework Membrane through Solution Processing for Pressureâ€Regulated Gas Separation. Angewandte Chemie, 2020, 132, 3868-3873.	2.0	20
205	Donor–acceptor covalent organic framework/g-C ₃ N ₄ hybrids for efficient visible light photocatalytic H ₂ production. Catalysis Science and Technology, 2021, 11, 2616-2621.	4.1	20
206	Synthesis of Water-Soluble Lanthanide Porphyrin Sandwich Complexes: Bis(tetrapyridylporphyrinato) Cerium(IV), [Ce(tpyp)2], and Bis(tetramethylpyridylporphyrinato) Cerium(IV), [Ce(tmpyp)2]. Bulletin of the Chemical Society of Japan, 1992, 65, 1990-1992.	3.2	19
207	Synthesis and liquid crystal behavior of tris[2,3,9,10,16,17,23,24-octakis(octyloxy)phthalocyaninato] rare earth complexes. Journal of Porphyrins and Phthalocyanines, 2007, 11, 100-108.	0.8	19
208	Methyloxy Substituted Heteroleptic Bis(phthalocyaninato) Yttrium Complexes: Density Functional Calculations. ChemPhysChem, 2008, 9, 781-792.	2.1	19
209	Synthesis, crystal structure and magnetic properties of a cyanide-bridged heterobimetallic trinuclear complex based on K[Cr(salen)(CN)2] building block. Inorganic Chemistry Communication, 2008, 11, 94-96.	3.9	19
210	Synthesis, structural characterization and cytotoxic activity of diorganotin(IV) complexes of <i>N</i> â€(5â€halosalicylidene)tryptophane. Applied Organometallic Chemistry, 2009, 23, 24-31.	3.5	19
211	Unprecedented cucurbituril-based ternary host–guest supramolecular polymers mediated through included alkyl chains. Polymer Chemistry, 2014, 5, 5211-5217.	3.9	19
212	Chiral benzo-fused Aza-BODIPYs with optical activity extending into the NIR range. Dyes and Pigments, 2016, 134, 427-433.	3.7	19
213	Structure and LIBs Anode Material Application of Novel Wells–Dawson Polyoxometalate-Based Metal Organic Frameworks with Different Helical Channels. Crystal Growth and Design, 2018, 18, 5564-5572.	3.0	19
214	Photonic Switching Porous Organic Polymers toward Reversible Control of Heterogeneous Photocatalysis. ACS Applied Materials & Interfaces, 2020, 12, 56491-56498.	8.0	19
215	Chiral porphyrin assemblies. Aggregate, 2023, 4, .	9.9	19
216	Sandwich-type mixed (phthalocyaninato)(porphyrinato) rare earth double-decker complexes with decreased molecular symmetry of Cs: Single crystal structure and self-assembled nano-structure. Dalton Transactions, 2011, 40, 107-113.	3.3	18

#	Article	IF	CITATIONS
217	Multiple correlations of mRNA expression and protein abundance in human cytokine profile. Molecular Biology Reports, 2014, 41, 6985-6993.	2.3	18
218	Low-temperature scanning tunneling microscopy study of double-decker DyPc ₂ on Pb Surface. Nanoscale, 2014, 6, 10779.	5.6	18
219	Unprecedented Phthalocyanines Bearing Eight Di-butylamino Peripheral Substituents: Synthesis, Spectroscopy, and Structure. Inorganic Chemistry, 2015, 54, 9962-9967.	4.0	18
220	Porous Pyrene Organic Cage with Unusual Absorption Bathochromic-Shift Enables Visible Light Photocatalysis. CCS Chemistry, 2022, 4, 2588-2596.	7.8	18
221	Raman spectroscopic characteristics of phthalocyanine and naphthalocyanine in sandwich-type phthalocyaninato and porphyrinato rare earth complexes. Part 5?Raman spectroscopic characteristics of naphthalocyanine in mixed [tetrakis(4-tert-butylphenyl)porphyrinato] (naphthalocyaninato) rare earth double-deckers. Journal of Raman Spectroscopy, 2003, 34, 306-314.	2.5	17
222	(Phthalocyaninato)copper(II) Complexes Fused with Different Numbers of 15-Crown-5 Moieties – Synthesis, Spectroscopy, Supramolecular Structures, and the Effects of Substituent Number and Molecular Symmetry. European Journal of Inorganic Chemistry, 2007, 2007, 3268-3275.	2.0	17
223	Unsymmetrical Pyreneâ€Fused Phthalocyanine Derivatives: Synthesis, Structure, and Properties. Chemistry - A European Journal, 2015, 21, 3168-3173.	3.3	17
224	Water Dispersible and Biocompatible Porphyrin-Based Nanospheres for Biophotonics Applications: A Novel Surfactant and Polyelectrolyte-Based Fabrication Strategy for Modifying Hydrophobic Porphyrins. ACS Applied Materials & Interfaces, 2015, 7, 19718-19725.	8.0	16
225	Detection and Manipulation of Charge States for Double-Decker DyPc ₂ Molecules on Ultrathin CuO Films. ACS Nano, 2018, 12, 2991-2997.	14.6	16
226	A phthalocyanine-porphyrin triad for ratiometric fluorescent detection of Lead(II) ions. Dyes and Pigments, 2020, 173, 107941.	3.7	16
227	Metal-free azo-bridged porphyrin porous organic polymers for visible-light-driven CO ₂ reduction to CO with high selectivity. Dalton Transactions, 2020, 49, 7592-7597.	3.3	16
228	Triptycene-supported bimetallic salen porous organic polymers for high efficiency CO ₂ fixation to cyclic carbonates. Inorganic Chemistry Frontiers, 2021, 8, 2880-2888.	6.0	16
229	Atomically Dispersed NiN ₃ Sites on Highly Defective Microâ€Mesoporous Carbon for Superior CO ₂ Electroreduction. Small, 2022, 18, e2107997.	10.0	16
230	Two-dimensional conjugated N-rich covalent organic frameworks for superior sodium storage. Science China Chemistry, 2022, 65, 1291-1298.	8.2	16
231	H ₂ O-Involved Hydrogen Bonds in Pseudo-Double-Decker Supramolecular Structure of 1,8,15,22-Tetrasubstituted Phthalocyaninato Zinc Complex. Crystal Growth and Design, 2008, 8, 4454-4459.	3.0	15
232	Recent Advances in Phthalocyanine-Based Functional Molecular Materials. Structure and Bonding, 2015, , 159-199.	1.0	15
233	Influence of porphyrin meso-attached substituent on the SMM behavior of dysprosium(iii) double-deckers with mixed tetrapyrrole ligands. RSC Advances, 2015, 5, 17732-17737.	3.6	15
234	Controlled morphology of self-assembled microstructures via solvent-vapor annealing temperature and ambipolar OFET performance based on a tris(phthalocyaninato) europium derivative. Dyes and Pigments, 2017, 143, 203-210.	3.7	15

#	Article	IF	CITATIONS
235	A porous tetraphenylethylene-based polymer for fast-response fluorescence sensing of Fe(III) ion and nitrobenzene. Dyes and Pigments, 2020, 173, 107929.	3.7	15
236	<i>cis</i> -Silicon phthalocyanine conformation endows <i>J</i> -aggregated nanosphere with unique near-infrared absorbance and fluorescence enhancement: a tumor sensitive phototheranostic agent with deep tissue penetrating ability. Journal of Materials Chemistry B, 2020, 8, 2895-2908.	5.8	15
237	A Robust Hydrogen-Bonded Organic Framework with 7-Fold Interpenetration Nets and High Permanent Microporosity. Crystal Growth and Design, 2022, 22, 1817-1823.	3.0	15
238	Nanoscale Hollow Spheres of an Amphiphilic Mixed (Phthalocyaninato)(porphyrinato)europium Doubleâ€Đecker Complex. European Journal of Inorganic Chemistry, 2010, 2010, 753-757.	2.0	14
239	Chiral bis(phthalocyaninato) yttrium double-decker complexes. Synthesis, structure, spectroscopy, and electrochemistry. Dalton Transactions, 2014, 43, 1699-1705.	3.3	14
240	Novel chiral ABBB-type unsymmetrical phthalocyanine. Ring-expansion synthesis, spectroscopic, and electrochemical properties. Dyes and Pigments, 2015, 120, 52-56.	3.7	14
241	Identification of heat shock protein 27 as a novel autoantigen of Behçet's disease. Biochemical and Biophysical Research Communications, 2015, 456, 866-871.	2.1	14
242	Nonperipheral Tetrakis(dibutylamino)phthalocyanines. New Types of 1,8,15,22-Tetrakis(substituted)phthalocyanine Isomers. Inorganic Chemistry, 2016, 55, 9289-9296.	4.0	14
243	Metformin enhances the osteogenesis and angiogenesis of human umbilical cord mesenchymal stem cells for tissue regeneration engineering. International Journal of Biochemistry and Cell Biology, 2021, 141, 106086.	2.8	14
244	A Solid Transformation into Carboxyl Dimers Based on a Robust Hydrogenâ€Bonded Organic Framework for Propyne/Propylene Separation. Angewandte Chemie, 2021, 133, 26146-26152.	2.0	14
245	Templated tetramerization of dicyanobenzenes to form mixed porphyrinato and phthalocyaninato rare earth(III) triple-decker complexes. Journal of Porphyrins and Phthalocyanines, 2002, 06, 347-357.	0.8	13
246	Heteroleptic protonated bis(phthalocyaninato) rare earth compounds containing 1,4,8,11,15,18,22,25-octa(butyloxy)-phthalocyanine ligand. Journal of Alloys and Compounds, 2006, 408-412, 1041-1045.	5.5	13
247	Synthesis and third-order nonlinear optical properties of novel ethynyl-linked heteropentamer composed of four porphyrins and one pyrene. Journal of Porphyrins and Phthalocyanines, 2009, 13, 275-282.	0.8	13
248	Sandwich-type (phthalocyaninato)(porphyrinato) europium triple-decker nanotubes. Effects of the phthalocyanine peripheral substituents on the molecular packing. Dalton Transactions, 2011, 40, 12895.	3.3	13
249	Intramolecular chirality induction and intermolecular chirality modulation in BINOL bridged bisporphyrin hosts. Dyes and Pigments, 2017, 137, 608-614.	3.7	13
250	Highly selective enzymatic-free electrochemical sensor for dopamine detection based on the self-assemblied film of a sandwich mixed (phthalocyaninato) (porphyrinato) europium derivative. Journal of Porphyrins and Phthalocyanines, 2017, 21, 796-802.	0.8	13
251	TTF-fused heteroleptic bis(phthalocyaninato) europium double-decker complexes. Synthesis, spectroscopic, and electrochemical properties. Dyes and Pigments, 2018, 156, 167-174.	3.7	13
252	Photoactive Porphyrinâ€Based Metalâ€Organic Framework Nanosheets. European Journal of Inorganic Chemistry, 2019, 2019, 4815-4819.	2.0	13

#	Article	IF	CITATIONS
253	Highly Efficient Multiphoton Absorption of Zincâ€AlEgen Metal–Organic Frameworks. Angewandte Chemie - International Edition, 2022, 61, .	13.8	13
254	Novel Pathway to Synthesize Unsymmetrical 2,3,9,10,16,17,23-heptakis(alkoxyl)-24-mono(dimethylaminoalkoxyl)phthalocyanines. Inorganic Chemistry, 2010, 49, 9005-9011.	4.0	12
255	Mixed (phthalocyanine)(Schiff-base) terbium(iii)–alkali metal(i)/zinc(ii) complexes: synthesis, structures, and spectroscopic properties. CrystEngComm, 2013, 15, 10383.	2.6	12
256	Constructing bis(porphyrinato) rare earth double-decker complexes involving N-confused porphyrin. Dalton Transactions, 2014, 43, 9152.	3.3	12
257	A Mixed Porphyrin–Schiff Base Dysprosium(III) Singleâ€Molecule Magnet. European Journal of Inorganic Chemistry, 2016, 2016, 4194-4198.	2.0	12
258	Heteroleptic Tetrapyrroleâ€Fused Dimeric and Trimeric Skeletons with Unusual Nonâ€Frustrated Fluorescence. Chemistry - A European Journal, 2016, 22, 4492-4499.	3.3	12
259	Synthesis, crystal structures, and fluorescence properties of porphyrin alkaline earth MOFs. Inorganic Chemistry Communication, 2018, 95, 36-39.	3.9	12
260	Bis[1,8,15,22-tetrakis(3-pentyloxy)phthalocyaninato]terbium Double-Decker Single-Ion Magnets. Inorganic Chemistry, 2019, 58, 2422-2429.	4.0	12
261	Manganese(III) Porphyrin-Based Magnetic Materials. Topics in Current Chemistry, 2019, 377, 18.	5.8	12
262	Dimeric phthalocyanine-involved double-decker complex-based electrochemical sensor for simultaneous detection of acetaminophen and ascorbic acid. Journal of Materials Science: Materials in Electronics, 2019, 30, 1976-1983.	2.2	12
263	Edge-located Fe-N4 sites on porous Graphene-like nanosheets for boosting CO2 electroreduction. Chemical Engineering Journal, 2022, 431, 134269.	12.7	12
264	Synthesis, crystal structure and magnetic properties of a new 2D cyanide-bridged heterobimetallic Cr(I)–Mn(III) complex. Inorganic Chemistry Communication, 2010, 13, 895-898.	3.9	11
265	Homobinuclear phthalocyaninato metal complexes. Synthesis, structure, spectroscopy, and electrochemistry. Dyes and Pigments, 2014, 109, 163-168.	3.7	11
266	A post-cyclotetramerization strategy towards novel binuclear phthalocyanine dimers. Inorganic Chemistry Frontiers, 2017, 4, 110-113.	6.0	11
267	Heteroleptic chiral bis(phthalocyaninato) terbium double-decker single-ion magnets. Inorganic Chemistry Frontiers, 2018, 5, 2006-2012.	6.0	11
268	Ferromagnetic coupling between 4f- and delocalized π-radical spins in mixed (phthalocyaninato)(porphyrinato) rare earth double-decker SMMs. Inorganic Chemistry Frontiers, 2019, 6, 2142-2147.	6.0	11
269	Unconventional dihydrogen-bond interaction induced cyanide-bridged chiral nano-sized magnetic molecular wheel: synthesis, crystal structure and systematic theoretical magnetism investigation. Journal of Materials Chemistry C, 2019, 7, 3623-3633.	5.5	11
270	An ultrafast BODIPY single molecular sensor for multi-analytes (acid/base/Cu2+/Bi3+) with different sensing mechanism. Dyes and Pigments, 2019, 165, 279-286.	3.7	11

#	Article	IF	CITATIONS
271	Sonochemical synthesis and fabrication of neodymium sesquioxide entrapped with graphene oxide based hierarchical nanocomposite for highly sensitive electrochemical sensor of anti-cancer (raloxifene) drug. Ultrasonics Sonochemistry, 2020, 64, 104717.	8.2	11
272	Multipolar Porphyrinâ€Triazatruxene Arrays for Twoâ€Photon Fluorescence Cell Imaging. Chemistry - A European Journal, 2020, 26, 13842-13848.	3.3	11
273	Ultralow loading of ruthenium nanoparticles on nitrogen-doped porous carbon enables ultrahigh mass activity for the hydrogen evolution reaction in alkaline media. Catalysis Science and Technology, 2021, 11, 3182-3188.	4.1	11
274	Covalent organic frameworks based on tetraphenyl- <i>p</i> -phenylenediamine and metalloporphyrin for electrochemical conversion of CO ₂ to CO. Inorganic Chemistry Frontiers, 2022, 9, 3217-3223.	6.0	11
275	Self-assembly and nonlinear optical properties of (μ-oxo)bis[meso-tetrakis(p-bromophenyl-porphyrinato)iron(<scp>iii</scp>)]. CrystEngComm, 2015, 17, 4699-4704.	2.6	10
276	ABAB-type phthalocyanines simultaneously bearing electron donating and electron accepting groups. Synthesis, spectroscopy, and structure. Inorganic Chemistry Frontiers, 2016, 3, 1146-1151.	6.0	10
277	Integration of inherent and induced chirality into subphthalocyanine analogue. Scientific Reports, 2016, 6, 28026.	3.3	10
278	Sensitivity enhancement of graphene Hall sensors modified by single-molecule magnets at room temperature. RSC Advances, 2017, 7, 1776-1781.	3.6	10
279	Alkali metal ions regulate the supramolecular chirality of interfacial assembly of achiral phthalocyanine. Dyes and Pigments, 2018, 157, 133-139.	3.7	10
280	A novel calix[4]arene-modified porphyrin-based dual-mode sensor for the specific detection of dopamine with excellent performance. New Journal of Chemistry, 2019, 43, 10376-10381.	2.8	10
281	Towards developing efficient aminopyridine-based electrochemical catalysts for CO2 reduction. A density functional theory study. Journal of Catalysis, 2019, 373, 75-80.	6.2	10
282	STM Investigation of the Y[C6S-Pc]2 and Y[C4O-Pc]2Complex at the Solution–Solid Interface: Substrate Effects, Submolecular Resolution, and Vacancies. Journal of Physical Chemistry C, 2021, 125, 1421-1431.	3.1	10
283	Enhanced Photocatalytic CO ₂ Reduction through Hydrophobic Microenvironment and Binuclear Cobalt Synergistic Effect in Metallogels. Angewandte Chemie - International Edition, 2022, 61, .	13.8	10
284	Electrochemistry of homoleptic bis[3(4),12(13),21(22),30(31)-tetra(<i>tert</i> -butyl)-naphthalocyaninato] rare earth(III) complexes. Journal of Porphyrins and Phthalocyanines, 2005, 09, 40-46.	0.8	9
285	Benzo-fused low symmetry metal-free tetraazaporphyrin and phthalocyanine analogs: synthesis, spectroscopy, electrochemistry, and density functional theory calculations. Journal of Porphyrins and Phthalocyanines, 2010, 14, 421-437.	0.8	9
286	Ring-Shaped J-Type and Star-Shaped H-Type Nanostructures of an Unsymmetrical (Phthalocyaninato)zinc Complex. European Journal of Inorganic Chemistry, 2011, 2011, 1466-1472.	2.0	9
287	Determination of Deoxynivalenol, Zearalenone, Aflatoxin B1, and Ochratoxin by an Enzyme-Linked Immunosorbent Assay. Analytical Letters, 2014, 47, 1912-1920.	1.8	9
288	Electron Transfer Flavoprotein Subunit Beta Is a Candidate Endothelial Cell Autoantigen in Behçet's Disease. PLoS ONE, 2015, 10, e0124760.	2.5	9

#	Article	IF	CITATIONS
289	Multinuclear Phthalocyanineâ€Fused Molecular Nanoarrays: Synthesis, Spectroscopy, and Semiconducting Property. Chemistry - A European Journal, 2017, 23, 8644-8651.	3.3	9
290	Sandwich rare earth complexes simultaneously involving aromatic phthalocyanine and antiaromatic hemiporphyrazine ligands showing a predominantly aromatic nature. Chemical Communications, 2017, 53, 3765-3768.	4.1	9
291	An AceDAN–porphyrin(Zn) dyad for fluorescence imaging and photodynamic therapy <i>via</i> two-photon excited FRET. Inorganic Chemistry Frontiers, 2018, 5, 3061-3066.	6.0	9
292	Hemiporphyrazine-Involved Sandwich Dysprosium Double-Decker Single-Ion Magnets. Inorganic Chemistry, 2018, 57, 12347-12353.	4.0	9
293	A sandwich-type tetrakis(phthalocyaninato) europium–cadmium quadruple-decker complex: structural, spectroscopic, OFET, and gas sensing properties. New Journal of Chemistry, 2019, 43, 15763-15767.	2.8	9
294	A calix[4]arene-modified (Pc)Eu(Pc)Eu[T(C4A)PP]-based sensor for highly sensitive and specific host–guest electrochemical recognition. Dalton Transactions, 2019, 48, 718-727.	3.3	9
295	Magnetic investigations over reversibly switched chiral (phthalocyaninato)(porphyrinato) dysprosium double-decker compounds. Dalton Transactions, 2019, 48, 1586-1590.	3.3	9
296	Controlling the Crystal Field of Heteroleptic Bis(phthalocyaninato) Erbium for Fieldâ€Induced Magnetic Relaxation. European Journal of Inorganic Chemistry, 2019, 2019, 2940-2946.	2.0	9
297	Atomic CoN3S1 sites for boosting oxygen reduction reaction via an atomic exchange strategy. Nano Research, 2022, 15, 1803-1808.	10.4	9
298	Co–Fe alloy nanoparticles and Fe3C nanocrystals on N-doped biomass-derived porous carbon for superior electrocatalytic oxygen reduction. Journal of Solid State Chemistry, 2022, 307, 122735.	2.9	9
299	Phthalocyanineâ€Triggered Helical Dipeptide Nanotubes with Intense Circularly Polarized Luminescence. Small, 2022, 18, e2104438.	10.0	9
300	Stimuli-Responsive Porous Molecular Crystal with Reversible Modulation of Porosity. ACS Applied Materials & Interfaces, 2022, 14, 1519-1525.	8.0	9
301	Synthesis and liquid crystal behavior of bis[3,4,12,13,21,22,30,31-octa(dodecylthio)-2,3-naphthalocyaninato] rare earth complexes. Journal of Porphyrins and Phthalocyanines, 2006, 10, 1132-1139.	0.8	8
302	POSS-based luminescent hybrid material for enhanced photo-emitting properties. Journal of Materials Science, 2013, 48, 7533-7539.	3.7	8
303	Vibrational spectroscopy of phthalocyanine and naphthalocyanine in sandwich-type (na)phthalocyaninato and porphyrinato rare earth complexes. Part 15: The IR characteristics of phthalocyanine in homoleptic tetrakis(phthalocyaninato) rare earth(III)-cadmium(II) quadruple-deckers. Vibrational Spectroscopy, 2013, 69, 8-12.	2.2	8
304	The electronic structures and charge transfer properties of tetra(naphthalene-dione)porphyrins and tetra(naphthalene-dithione)porphyrins as dye-sensitized solar cell skeleton. International Journal of Quantum Chemistry, 2013, 113, 2605-2610.	2.0	8
305	Unraveling the formation mechanism of subphthalocyanine. Density functional theory studies. Inorganic Chemistry Communication, 2017, 85, 9-15.	3.9	8
306	Heterobimetallic complexes from 0D clusters to 3D networks based on various polycyanometallates and [Cu(dmpn) ₂] ²⁺ (dmpn = 2,2-dimethyl-1,3-diaminopropane): synthesis, crystal structures and magnetic properties. CrystEngComm, 2020, 22, 2806-2816.	2.6	8

#	Article	IF	CITATIONS
307	Cobalt Nanocluster-Decorated N-Rich Hierarchical Carbon Architectures Efficiently Catalyze Oxygen Reduction and Hydrogen Evolution Reactions. ACS Sustainable Chemistry and Engineering, 2022, 10, 2001-2009.	6.7	8
308	Sensitive and selective sensor based on porphyrin porous organic cage fluorescence towards copper ion. Dyes and Pigments, 2022, 200, 110117.	3.7	8
309	Enantioselective assembly and recognition of heterochiral porous organic cages deduced from binary chiral components. Chemical Science, 2022, 13, 7014-7020.	7.4	8
310	A new series of cyanide-bridged heterobimetallic FeIII–FeIII/MnIII/CuII one-dimensional complexes: synthesis, crystal structures, and magnetic properties. New Journal of Chemistry, 2014, 38, 5470-5479.	2.8	7
311	The first porphyrin–subphthalocyaninatoboron(<scp>iii</scp>)-fused hybrid with unique conformation and intramolecular charge transfer behavior. Chemical Communications, 2016, 52, 10517-10520.	4.1	7
312	Phenanthro[4,5â€ <i>fgh</i>]quinoxalineâ€Fused Subphthalocyanines: Synthesis, Structure, and Spectroscopic Characterization. Chemistry - A European Journal, 2016, 22, 9488-9492.	3.3	7
313	An indirect ELISA-inspired dual-channel fluorescent immunoassay based on MPA-capped CdTe/ZnS QDs. Analytical and Bioanalytical Chemistry, 2019, 411, 5437-5444.	3.7	7
314	Compartmentalization within Nanofibers of Doubleâ€Decker Phthalocyanine Induces Highâ€Performance Sensing in both Aqueous Solution and the Gas Phase. Chemistry - A European Journal, 2019, 25, 16207-16213.	3.3	7
315	Advances in gas sensors of tetrapyrrolato-rare earth sandwich-type complexes — CommemoratingÂtheÂ100thÂanniversaryÂofÂtheÂbirthÂofÂAcademicianÂGuangxianÂXu. Journal of Rare Earths, 2021, 39, 113-120.	4.8	7
316	Calreticulin as a special marker to distinguish dental pulp stem cells from gingival mesenchymal stem cells. International Journal of Biological Macromolecules, 2021, 178, 229-239.	7.5	7
317	High Fluorescence Porous Organic Cage for Sensing Divalent Palladium Ion and Encapsulating Fine Palladium Nanoparticles. Chinese Journal of Chemistry, 2022, 40, 385-391.	4.9	7
318	F-doped carbon hollow nanospheres for efficient electrochemical oxygen reduction. Journal of Materials Science, 2022, 57, 5924-5932.	3.7	7
319	Metallomacrocycle-supported interpenetration networks assembled from binary N-containing ligands. CrystEngComm, 2016, 18, 3506-3512.	2.6	6
320	Novel chiral binaphthalene-linked pyrenes. Synthesis, structure, and spectroscopy. Dyes and Pigments, 2017, 141, 245-250.	3.7	6
321	Novel, linear oligoisoindole compounds with a conjugated electronic structure. Organic Chemistry Frontiers, 2017, 4, 2364-2369.	4.5	6
322	Room temperature chiral reorganization of interfacial assembly of achiral double-decker phthalocyanine. Physical Chemistry Chemical Physics, 2018, 20, 7223-7229.	2.8	6
323	Regulating the emission of tetraphenylethenes by changing the alkoxyl linkage length between two neighboring phenyl moieties. Chemical Communications, 2018, 54, 6987-6990.	4.1	6
324	Solution-processable (Pc′)Eu(Pc′)Eu[TP(OH)PP]/rGO bilayer heterojunction organic transistors with exceptional excellent ambipolar performance. Journal of Materials Science: Materials in Electronics, 2019, 30, 12437-12446.	2.2	6

#	Article	IF	CITATIONS
325	A porphyrin-pyranine dyad for ratiometric fluorescent sensing of intracellular pH. Journal of Photochemistry and Photobiology A: Chemistry, 2020, 396, 112524.	3.9	6
326	An efficient strategy to boost the directed migration of photogenerated holes by introducing phthalocyanine as a hole extraction layer. Inorganic Chemistry Frontiers, 2022, 9, 3915-3923.	6.0	6
327	Peripheryâ€Hydrogenating Effects on the Unordinary 14 Ï€â€Electron Delocalized Circuits and Related Electronic Properties of Subporphyrazine Analogs: A Density Functional Theory Investigation. Chinese Journal of Chemistry, 2012, 30, 2126-2130.	4.9	5
328	Experimental and Theoretical Characterization of 5,10â€Diminoporphodimethenes: Dearomatized Porphyrinoids from Palladiumâ€Catalyzed Hydrazinations of 5,10â€Diarylporphyrins. ChemPlusChem, 2014, 79, 813-824.	2.8	5
329	Unprecedented phthalocyanine–porphyrin-fused oligomers with induced chirality nature. Inorganic Chemistry Frontiers, 2017, 4, 104-109.	6.0	5
330	An Azacrown[N,S,O]–Styryl Modified Boron–Phenylpyrrin: Coordinationâ€Modeâ€Transitionâ€Induced Colorimetric and OFF–ON–OFF Fluorescence Chemosensor for Quantifying Cu ²⁺ . European Journal of Inorganic Chemistry, 2017, 2017, 5254-5259.	2.0	5
331	Molecular assembly-induced charge transfer between a mixed (phthalocyaninato)(porphyrinato) yttrium triple-decker and a fullerene. Inorganic Chemistry Frontiers, 2019, 6, 654-658.	6.0	5
332	High mobility at the interface of the cocrystallized sandwich-type tetrapyrrole metal compound and fullerene layers. Inorganic Chemistry Frontiers, 2019, 6, 3345-3349.	6.0	5
333	Elucidating ï€â€"ï€ interaction-induced extension effect in sandwich phthalocyaninato compounds. RSC Advances, 2020, 10, 317-322.	3.6	5
334	Ethylthio-substituted sandwich phthalocyaninato europium (III) semiconductors for sensing NO2 and NH3: Effect of the extended ï€-conjugate systems on tuning the conductivity and sensing behavior. Organic Electronics, 2021, 93, 106151.	2.6	5
335	Cocatalystâ€Free Reduction of 4,4′â€Dinitrodiphenyl Ether to 4,4′â€Diaminodiphenyl Ether Over Twinâ€Cry Zn _x Cd _{1â^'x} S under Visible Light. ChemCatChem, 2021, 13, 4591-4601.	vstal 3.7	5
336	Efficient hydrogenation of cinnamaldehyde to 3-phenylpropanol on Ni/NiS-modified twin Zn _{0.5} Cd _{0.5} S under visible light irradiation. Catalysis Science and Technology, 2022, 12, 3706-3715.	4.1	5
337	Ordered supramolecular assembly of bis[3,4,1 2,13,21,22,30, 31-octa(dodecylthio)-2,3-naphthalocyaninato] erbium at the air/water interface. Science in China Series B: Chemistry, 2001, 44, 650-656.	0.8	4
338	Density functional theory study on organic semiconductor for field effect transistors: Symmetrical and unsymmetrical porphyrazine derivatives with annulated 1,2,5-thiadiazole and 1,4-diamyloxybenzene moieties. Science in China Series B: Chemistry, 2009, 52, 840-848.	0.8	4
339	A novel photochromic and electrochromic europium tetraazaporphyrinato and phthalocyaninato heteroleptic double-decker for information storage. Journal of Porphyrins and Phthalocyanines, 2009, 13, 1197-1205.	0.8	4
340	Combinatorial experimental and DFT theoretical investigation over the formation mechanism of a binuclear phthalocyanine dimer. RSC Advances, 2017, 7, 53043-53047.	3.6	4
341	Distribution of the unpaired electron in neutral bis(phthalocyaninato) yttrium double-deckers: An experimental and theoretical combinative investigation. Journal of Porphyrins and Phthalocyanines, 2018, 22, 165-172.	0.8	4
342	Vibrational spectra of alkylamino substituted phthalocyanine compounds: Density functional theory calculations. Journal of Porphyrins and Phthalocyanines, 2018, 22, 771-776.	0.8	4

#	Article	IF	CITATIONS
343	Quintuple-Decker Heteroleptic Phthalocyanine Heterometallic Samarium–Cadmium Complexes. Synthesis, Crystal Structure, Electrochemical Behavior, and Spectroscopic Investigation. Inorganic Chemistry, 2020, 59, 17591-17599.	4.0	4
344	An anionic potassium-organic framework for selective removal of uranyl ions. Dalton Transactions, 2021, 50, 8314-8321.	3.3	4
345	Heterogeneous Nuclear Ribonucleoprotein A2/B1 as a Target Antigen in Han Chinese for BD Patients. Protein and Peptide Letters, 2015, 22, 504-508.	0.9	4
346	Transplantation of feces from mice with Alzheimer's disease promoted lung cancer growth. Biochemical and Biophysical Research Communications, 2022, 600, 67-74.	2.1	4
347	Cyanide-bridged complexes based on dinuclear Cu(II)-M(II) [M = Pb and Cu] building blocks: Synthesis, crystal structures and magnetic properties. Science China Chemistry, 2012, 55, 978-986.	8.2	3
348	An unprecedented porphyrin-pillar[5]arene hybrid ditopic receptor. RSC Advances, 2015, 5, 43218-43224.	3.6	3
349	Crown-ether-substituted asymmetric phthalocyanine derivatives/CdS self-assembled hybrid films with an unprecedented high response toward NO2. Journal of Porphyrins and Phthalocyanines, 2019, 23, 507-517.	0.8	3
350	Unique electronic structure of Tri-μ-oxido-[bis(porphyrinato)niobium(V)]: Spontaneous symmetry breaking mechanism of the special coordination skeleton. Computational and Theoretical Chemistry, 2020, 1181, 112832.	2.5	3
351	Spin Crossover in a Series of Non-Hofmann-Type Fe(II) Coordination Polymers Based on [Hg(SeCN) ₃] ^{â°i} or [Hg(SeCN) ₄] ^{2–} Building Blocks. Inorganic Chemistry, 2021, 60, 11048-11057.	4.0	3
352	Magnetic Behaviors and Nonlinear Optical Properties of Heteroleptic Bis(phthalocyaninato) Holmium Compounds. European Journal of Inorganic Chemistry, 2021, 2021, 3512-3516.	2.0	3
353	Mesoporous Polyimideâ€ŀinked Covalent Organic Framework with Multiple Redoxâ€active Sites for Highâ€Performance Cathodic Li Storage. Angewandte Chemie, 0, , .	2.0	3
354	Structures and properties of novel 5,15-di[4-(5-acetylsulfanylpentyloxy)phenyl] porphyrin derivatives: Density functional theory calculations. Science China Chemistry, 2010, 53, 2183-2192.	8.2	2
355	Tetrakis(phthalocyaninato) terbium–cadmium quadruple-decker liquid crystals with good semiconducting properties. Organic Electronics, 2014, 15, 2654-2660.	2.6	2
356	Towards Clarifying the Role of O ₂ during the Phthalocyanine Synthesis. Chemistry - A European Journal, 2015, 21, 18461-18465.	3.3	2
357	New Meso-ortho-hydroxy-decorating Fluorescent ON-OFF Bodipy sensor to Cu2+. Inorganic Chemistry Communication, 2016, 68, 9-12.	3.9	2
358	Controlled preparation of ZnS nanoparticle arrays in Langmiur monolayer of an unsymmetrical phthalocyaninato zinc complex: Synthesis, organization and semiconducting properties. Journal of Porphyrins and Phthalocyanines, 2016, 20, 1334-1341.	0.8	2
359	Single-Ion Magnet Investigation of ABAB-Type Tetrachloro- and Tetraalkoxy-Substituted Bis(phthalocyaninato) Terbium Double-Decker with D 2 Symmetrical Ligand Field. European Journal of Inorganic Chemistry, 2019, 2019, 1329-1334.	2.0	2
360	A sextuple-decker heteroleptic phthalocyanine heterometallic samarium–cadmium complex with crystal structure and nonlinear optical properties in solution and gel glass. Dalton Transactions, 2021, 50, 13661-13665.	3.3	2

#	Article	IF	CITATIONS
361	Nature of the near-IR band in the electronic absorption spectra of neutral bis(tetrapyrrole) rare earth(III) complexes: Time-dependent density functional theory calculations. International Journal of Quantum Chemistry, 2010, 110, 1559-1564.	2.0	1
362	Synthesis, characterization and cytotoxic activity of 5,10,15,20â€ŧetrakis[4â€﴿triorganostannyloxy)phenyl]porphyrins. Applied Organometallic Chemistry, 2013, 27, 191-197.	3.5	1
363	Mixed Phthalocyanine–Porphyrin Fused Conjugated Pentameric Nanoarrays. Chemistry - A European Journal, 2017, 23, 15017-15021.	3.3	1
364	Air–water interfacial assembly of all-aromatic-substituted double-decker phthalocyanine forms aligned nanoparticles. Journal of Porphyrins and Phthalocyanines, 2018, 22, 791-798.	0.8	1
365	An Overall Comprehension of Antiâ€Aromatic Porphyrinoids Using 3Dâ€Graphical Chemical Shielding Description. Advanced Theory and Simulations, 2020, 3, 2000007.	2.8	1
366	Photophysical Behaviors of Shape-persistent Zinc Porphyrin Organic Cage. New Journal of Chemistry, 0, , .	2.8	1
367	Highly efficient bifunctional catalyst with 2D MoN formed in situ synergy for OER and ORR based-on Co(II) doped Mo(IV)-Ni(II) supramolecular coordination polymer. Molecular Catalysis, 2022, 528, 112513.	2.0	1
368	Praseodymium bis[phthalocyaninato] complex based gas sensor using a charge-flow transistor. Journal of Materials Science Letters, 2001, 20, 1009-1011.	0.5	0
369	Optically Active Mixed Phthalocyaninato-porphyrinato Rare-Earth Double-Decker Complexes: Synthesis, Spectroscopy, and Solvent-Dependent Molecular Conformation. Chemistry - A European Journal, 2008, 14, 6288-6288.	3.3	Ο
370	Organic photovoltaic cells made from phthalocyanine deckers. Conference Record of the IEEE Photovoltaic Specialists Conference, 2008, , .	0.0	0
371	Charge transfer properties of phthalocyaninato zinc complexes for organic field-effect transistors: tuning semiconductor nature <i>via</i> peripheral substituents. Journal of Porphyrins and Phthalocyanines, 2011, 15, 964-972.	0.8	Ο
372	Multiple Foreign Gene Delivery Can Induce Antibody Production in Mice. Analytical Letters, 2012, 45, 2066-2074.	1.8	0
373	Experimental and Theoretical Characterization of 5,10-Diminoporphodimethenes: Dearomatized Porphyrinoids from Palladium-Catalyzed Hydrazinations of 5,10-Diarylporphyrins. ChemPlusChem, 2014, 79, 752-752.	2.8	Ο
374	Frontispiece: Unsymmetrical Pyreneâ€Fused Phthalocyanine Derivatives: Synthesis, Structure, and Properties. Chemistry - A European Journal, 2015, 21, .	3.3	0
375	Raman spectra of rare earth double-decker complexes with porphyrinato and 2,3-naphthalocyaninato ligands. Journal of Porphyrins and Phthalocyanines, 2019, 23, 260-266.	0.8	Ο
376	Innentitelbild: Fabrication of a Hydrogenâ€Bonded Organic Framework Membrane through Solution Processing for Pressureâ€Regulated Gas Separation (Angew. Chem. 10/2020). Angewandte Chemie, 2020, 132, 3778-3778.	2.0	0
377	Crown-ether-substituted asymmetric phthalocyanine derivatives/CdS self-assembled hybrid films with an unprecedented high response toward NO2. , 2021, , 1020-1030.		0
378	High-selective room-temperature NO2 sensors based on a coumarin-substituted tris(phthalocyaninato) europium. Journal of Porphyrins and Phthalocyanines, 0, , A-G.	0.8	0

#	Article	IF	CITATIONS
379	Titelbild: Highly Efficient Multiphoton Absorption of Zincâ€AlEgen Metal–Organic Frameworks (Angew.) Tj l	ETQq110.7	'84314 rgBT /C
380	Highly Efficient Multiphoton Absorption of Zincâ€AlEgen Metal–Organic Frameworks. Angewandte Chemie, 0, , .	2.0	0
381	Enhanced Photocatalytic CO2 Reduction through Hydrophobic Microenvironment and Binuclear Cobalt Synergistic Effect in Metallogels. Angewandte Chemie, 0, , .	2.0	Ο